UDC 542.65

Determination of the Physicochemical Characteristics and Biological Activity *in vitro* of the Composite Ca–P/Chitosan Coating Obtained by Means of Electrochemical Deposition

YA. A. KAMENCHUK[1], E. A. ZELICHENKO[2], V. V. GUZEEV[1], A. B. SHASHKIN[2], I. A. KHLUSOV[1] and K. V. ZAITSEV[1]

[1]*Russian Ilizarov Scientific Center for Restorative Traumatology and Orthopaedics, Tomsk Branch, Ul. Nikitina 17, Tomsk 634034 (Russia)*

E-mail: Yana100@inbox.ru

[2]*Biotekhnika Co., Per. Plekhanova 5, Tomsk 634034 (Russia)*

(Received October 28, 2009; revised February 19, 2010)

Abstract

Physicochemical and biological properties of the composite calcium phosphate chitosan coating are investigated. It is shown that the introduction of chitosan increases the concentration of the amorphous phase composed of nanosized particles; an increase in its concentration leads to changes of the thickness and roughness of the coating. It was revealed that during obtaining the composite coating by means of electrochemical deposition, chitosan and Ca–P get deposited onto the surface of titanium substrate interchanging chaotically and mutually supplementing each other, with the formation of a net structure. The CaP/Ch composites modulate *in vitro* and *in vivo* the functional activity and differentiation of stromal stem cells in the osteogenic direction, due to which they are promising in the aspect of developing new class of implants for orthopaedics and traumatology.

Key words: chitosan, hydroxyapatite, electrochemical deposition, composite coating, stromal stem cells, osteogenic properties

INTRODUCTION

Among inorganic non-metal materials for making implants, materials based on hydroxyapatite are most widespread. Attention to hydroxyapatite (HA) is caused by its similarity in physicochemical properties with the mineral component of bone tissue and high biological activity. It was assumed that the addition of chitosan would increase biocompatibility of the Ca–P coating obtained using the electrochemical method [1].

Chitosan is the product of deacetylation of chitin, which is a biopolymer occurring in the skeleton tissues of insects and crustaceans [2, 3].

Chitosan is known as a hemostatic, fungistatic, immunomodulator, it possesses anti-tumour effect, and it is a natural biopolymer and is fully compatible with the tissues of an organism, which allows using it in many areas of medicine [4–6]. Moreover, chitosan is metabolized by a number of enzymes, in particular lysosomes, and is considered as biodegradable [7, 8]. Due to the positive charges in the case of physiological pH, chitosan is bioadhesive, which increases retention of cells [9, 10]. Chitosan also stimulates wound healing [11, 12] and exhibits bacteriostatic effect [13, 14].

EXPERIMENTAL

Obtaining composite coatings based on Ca–P with chitosan (Ca–P/Ch)

Composite coatings were obtained by electrochemical deposition. The substrate for coating deposition was a titanium alloy of VT 6 grade. Discs 9 mm in diameter, 2 mm thick with

TABLE 1

Conditions of deposition of Ca–P/chitosan coatings

Conditions	Ca–P	Ca–P/Ch1	Ca–P/Ch2
Temperature, °C	28–30	28–30	28–30
Time, min	15	25	25
pH of electrolyte solution	2.8–3.2	3.0–3.2	3.0–3.2
Density of pulsed current, mA/cm^2	0.1–0.2	0.1–0.2	0.1–0.2
Pulse repetition frequency, pulses/min	50–100	50–100	50–100
Chitosan concentration, g/L	0	1.25	5

the roughness of 2.5 mm were manufactured. Before depositing the coatings, the discs were washed using ultrasound in distilled water. Chitosan (deacetylation degree 85 %) in the concentrations of 1.25, 2 and 5 g/L) were added to the electrolyte containing calcium orthophosphates and phosphoric acid. The conditions of deposition are presented in Table 1.

After deposition of coatings, the samples were washed with distilled water and dried in the air in a desiccator at a temperature of 60–70 °C for 10–15 min.

The model culture to study the interaction of artificial coatings with stromal stem cells *in vitro* was fibroblast-like cells of human lungs (LLC Stem Cell Banking) that were cloned in the osteogenic medium [15] on discs with coating, 9 mm in diameter, in the concentration of $5 \cdot 10^4$ cells/cm^2 for 4 days. Preparations after 4–5 passages are morphologically and functionally uniform cell populations with limited lifetime, conserving stable karyotype during passages. The cells are free from foreign viruses (HIV, hepatitis, herpes *etc.*) and bacterial agents (syphilis, mycoplasmas, chlamydia *etc.*). The vital capacity of the cells, determined according to ISO 10993-5 on the basis of the absence of colouring in the test with 0.4 % trypan blue, was 91–93 %.

After the end of culturing, the implants were dried in the air, adherent cell material was fixed for 30 s in formalin vapour, coloured for alkaline phosphatase (AP) according to the procedure described in [16].

In the experiment *in vivo, we* introduced one implant per an individual into male mice of the Balb/c line (implant diameter: 9 mm, thickness: 2 mm); a column of syngeneic bone marrow taken from the femoral bone was deposited under aseptic conditions onto each implant (osteogenesis test). For cell adhesion, the organ culture of bone marrow on the substrate was cultivated for 45 min in the culture medium containing 95 % RPMI-1640 (ICN) medium and 5 % embryonic calf serum (ICN). Bone marrow served as the source of multipotent mesenchymal stromal cells (MMSC) and growth factors. No formation of tissue plates was observed after separate subcutaneous introduction of substrates or the fragments of bone marrow into mice.

After 45 days implants were extracted, photographed in the reflected light with fixed parameters. To carry out histological analysis, we used standard methods of light microscopy of thin sections. After decalcification of tissue plates grown on implants, usual hematoxylin and eosin stain for paraffin sections made perpendicularly to the disc surface was performed.

TABLE 2

Characterization of sample surface (n = 5)

Conditions	Ca–P	Ca–P/Ch1	Ca–P/Ch2
Chitosan concentration in the electrolyte solution, g/L	0	1.25	5
Thickness of coating, μm	85± 3.0	81±2	60±2.0
Surface roughness, μm	5.5±0.2	4.7±0.1	4.0±0.1

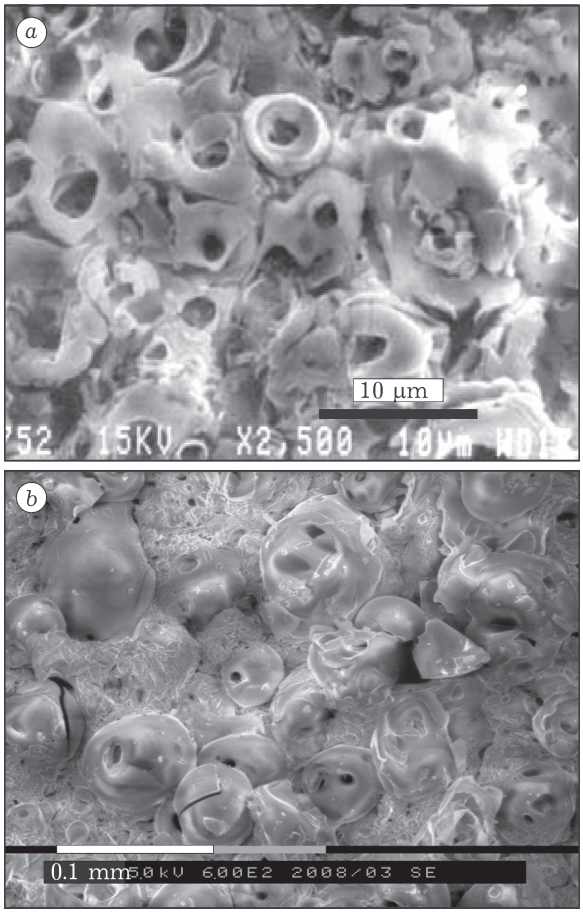

Fig. 1. Microphotographs of Ca–P (*a*) and Ca–P/Ch (5 g/L chitosan in solution) coatings (*b*), according to the SEM data.

RESULTS AND DISCUSSION

Studies of surface topography

The thickness of coatings was determined by a Konstanta K5 polyfunctional device. Measurement results ($n = 5$) showed that an increase in the concentration of chitosan in solution causes a decrease in the thickness of coatings (Table 2). Surface roughness was determined using the optical microscope with built-in profilometer OMP-0360G. Measurement results provide evidence that the roughness decreases with an increase in chitosan concentration (see Table 2).

The micro- and macro-relief of the surface of coatings was studied with a Philips SEM 515 scanning electron microscope. The Ca–P and Ca–P/Ch coatings were formed from Ca–P globules with the diameter of 80 nm to 150 μm. The Ca–P coating was composed of spherulite-like crystals forming the macro-relief of surface with pore size within the range 5–100 μm. Isolated pores were localized in spherulites; through pores were located at the boundaries of spherulites. The Ca–P/Ch coatings were also formed from spherulites, but the surface relief looked smoother due to wrapping the globules of calcium phosphate with chitosan, with the average pore size about 15 μm. On the

TABLE 3

Phase composition of Ca–P and Ca–P/Ch2 coatings

Samples	Detected phases	Volume concentration of phase, %	Lattice parameters, Å	Average particle size, nm	$\Delta d/(d \cdot 10^{-3})$
Ca–P	$Ca_5(PO_4)_3(OH)$	66.3	a = 9.4083	300	0.5
			c = 6.8777		
	Ti	1.5	a = 2.9354	16	2.7
			c = 4.6571		
	TiO_2 – brookite	2.2	a = 9.1139	9	8.5
			b = 5.4729		
			c = 5.1679		
	Amorphous	30	–	–	–
Ca–P/Ch2	$Ca_5(PO_4)_3(OH)$	25	a = 9.4083	30	19
			c = 6.8777		
	TiO_2 – brookite	15	a = 9.1139	22	10
			b = 5.4729		
			c = 5.1679		
	Amorphous	60	–	–	–

Ca–P/Ch coating, the majority of polymer aggregates both concentrate around Ca–P globules and cover them. Sometimes Ca–P binding to chitosan with the formation of a meshwork was detected (Fig. 1, *b*). In the Ca–P coating we detected Ca–P globules looking like spherulites. Chitosan aggregates concentrated around Ca–P globules and connected with each other, thus forming a meshwork, were detected in Ca–P/Ch2 coating.

Examination of the phase composition and parameters of the structure of coatings was carried out on a Shimadzu XRD-6000 diffractometer (CuK_α radiation). Analysis of the phase composition, coherent length, and internal elastic strain was carried out using the PCPDFWIN databases and the program of full-profile analysis POWDER CELL 2.4.

The Ca–P coating exhibits typical apatite peaks with the crystallinity about 66.3 % and admixture of the amorphous phase (30 %). The addition of chitosan (Ca–P/Ch2 coating) caused a decrease in the content of the crystalline apatite phase to 25 % and an increase in the content of the amorphous phase (60 %) and brushite phase (15 %). After the introduction of chitosan, the size of crystallites forming spherulites decreases substantially (Table 3).

Composition and structure of the coating

The composition of the coatings was studied with a Specord M 80 spectrophotometer (Fig. 2). The IR spectrum of chitosan contains broad absorption bands between 1079 and 1032 cm^{-1}, corresponding to the glycoside bond C–O–C, and a peak at 1260 cm^{-1}, attributed to the free primary amino group (NH_2) in position C_2 of glucosamine. The peak at 3439 cm^{-1} relates to the vibrations of OH groups in adsorbed water. The peak at 1655 cm^{-1} (amide 1) with a small shoulder and the peak at 1605 cm^{-1} (amide 2) relate to acetylated amino group and confirm incomplete deacetylation of the sample. The peak at 1381 cm^{-1} corresponds to C–O bond of the primary alcohol groups ($-CH_2-OH$). In addition, weak absorption bands at 896 and 664 cm^{-1} are present; they can be assigned to the bending vibrations of C_1–H group and the vibrations of the pyranose ring in β-carbohydrates, respectively. The spectra also

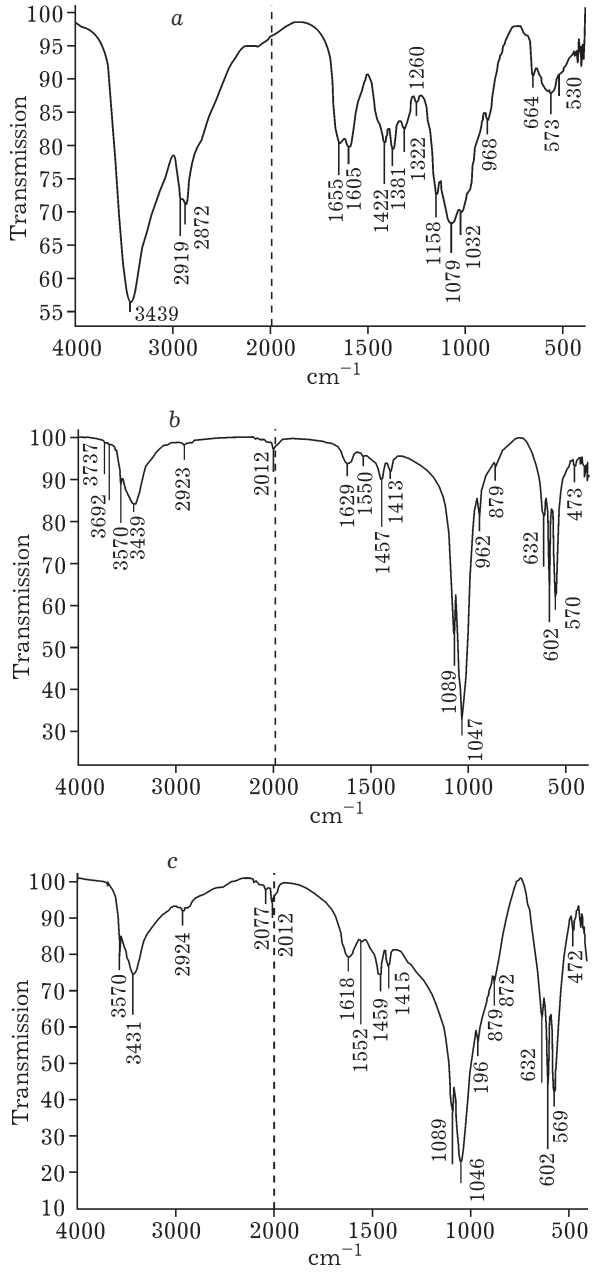

Fig. 2. IR spectra of chitosan (*a*), hydroxyapatite (*b*), and Ca–P/Ch2 (*c*).

contain absorption bands related to the aliphatic groups CH_2 (2919 cm^{-1}) and CH_3 (2872 cm^{-1}), which is indicated by the presence of bands corresponding to the bending vibrations of these groups at 1422 and 1322 cm^{-1}.

The IR spectrum of hydroxyapatite contains absorption bands within the frequency region 570, 602 cm^{-1}, which are attributed to the bending vibrations of P–O bonds; the band at 632 cm^{-1} relates to the bending vibrations of OH groups at 6_3 axes; the band at 962 cm^{-1}

relates to the ν_1 vibrations of P–O bonds. The bands appearing at 1047–1089 cm^{-1} are the characteristic vibrations of phosphate.

The IR spectrum of the Ca–P/Ch2 composite demonstrates all the characteristic absorption bands for hydroxyapatite and chitosan. A broad absorption band at 3431 cm^{-1} corresponds to the stretching vibrations of OH groups, while absorption peaks at 2924 cm^{-1} relate to aliphatic groups C–H. No shifts of absorption bands are observed in the spectrum of the composite, therefore, no chemical bonds are formed between chitosan and hydroxyapatite, that is, they are combined only mechanically.

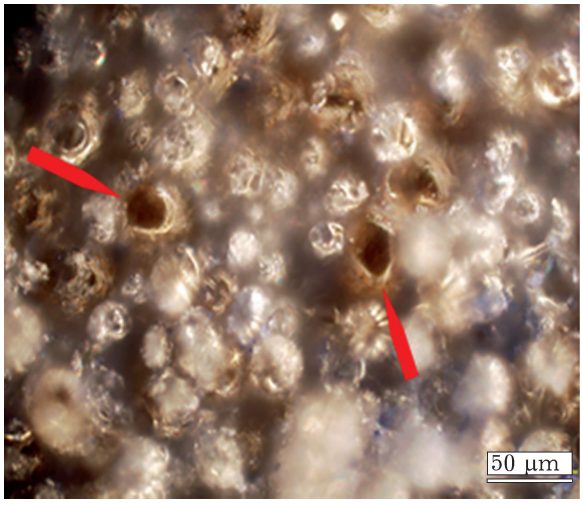

Fig. 3. Surface of Ca–P/Ch2 composites coloured for alkaline phosphatase. Arrows show the sites where positively coloured cells are situated.

Biological properties of coatings

The results of culturing of the stromal stem cells on the implants under study showed that the cells positively coloured at AP are situated in the pores of the coating (Fig. 3). Alkaline phosphatase is considered to be the marker of osteoblasts [17] differentiating during culturing from stromal stem cells. Our results show that the majority of stromal cells of bone marrow join the Ca–P/Ch2 coating after the first two days of culturing.

We established that the cells mainly get bound to chitosan. These data indicate that the Ca–P/Ch2 coating is more efficient for the attachment of the stromal cells of bone marrow than the Ca–P coating. The obtained results also confirm our hypothesis that the biocompatibility undoubtedly increases with the addition of chitosan. This fact is connected with the structural changes of the Ca–P coating. There is an assumption that the chemical structure of chitosan is similar to glycosaminoglycan, the key molecule of extracellular fluid controlling the morphology and function of cells [18]. Due to this similarity, chitosan can provide the addition of cell. The results of the tests of ectopic osteogenesis showed that the

TABLE 4

Test of ectopic osteogenesis for Ca–P and Ca–P/Ch2 coatings

Sample No.	Inflammation	Implant encapsulation	Tissue plate	Histology
			Ca–P/Ch2	
1	–	–	+	Bone with marrow
2	–	–	+	Bone with marrow
3	–	–	+	Bone (girder) with marrow
4	–	–	+	Bone weak
			Ca–P	
1	–	–	+	Connective tissue
2	–	–	+	Woven bone + marrow Major matter of bone is immature on the coating
3	–	–	+	Woven bone + marrow Major matter of bone is immature on the coating
4	–	–	+	Woven bone + marrow Major matter of bone is immature on the coating

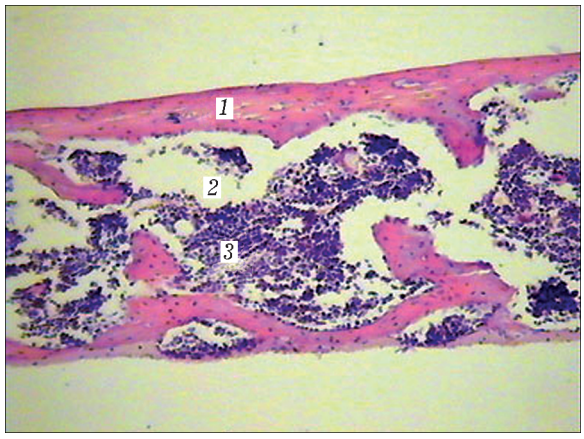

Fig. 4. Cross section of the tissue plate grown on the Ca–P/Ch2 coating in the test of ectopic histogenesis: *1* – bone tissue, *2* – medullary cavities filled with bone marrow (*3*). Coloured with hematoxylin-eosine.

introduction of chitosan increases the probability of bone growth up to 10 % (Table 4). The results of histological analysis of implants after their extraction from mice point to the formation of bone tissue (Fig. 4).

SUMMARY

1. It was revealed that the introduction of chitosan causes smoothing of the surface relief of coating due to chitosan wrapping of the globules of calcium phosphate. Sometimes binding of Ca–P with chitosan occurs, with the formation of a meshwork structure.

2. The addition of chitosan causes a decrease in the content of crystal apatite phase and an increase in the content of both the amorphous and brushite phases. After the introduction of chitosan, the size of crystallites forming spherulites decrease substantially.

3. The spectrum of the composite does not exhibit any shifts of absorption bands, therefore, no chemical bonds are formed between chitosan and hydroxyapatite, and that is, they are combined only mechanically.

4. The Ca–P/Ch composites modulate *in vitro* and *in vivo* functional activity and differentiation of stromal stem cells in the direction of osteogenesis.

REFERENCES

1 Zhogolev K. D., Nikitin V. Yu., Tsygan E. N., Knyazkin I. V., Kotik N. S., Egorov V. N., Pakhomov E. Yu., Regulyatsiya Osteogeneza i Immunogeneza Reparativnykh Protsessov, Izd-vo VMA, St. Petersburg, 2003, pp. 54–60.
2 Sorlier P., Denuziere A., Viton C., Domard A., *Biomacromol.*, 2 (2001) 765.
3 Dong Y. M., Qiu W. B., Ruan Y. H., Wu Y. S., Wang M. A., Xu C.Y., *Polym. J.*, 33 (2001) 387.
4 Felt O., Furrer P., Mayer J. M., Plazonnet B., Buri P., Gurny R., *Int. J. Pharm.*, 180 (1999) 185.
5 Patashnik S., Rabinovich L., Golomb G., *J. Drug Targ.*, 4 (1997) 371.
6 Song J. S., Such C. H., Park Y. B., Lee S. H., Yoo N. C., Lee J. D., Kim K. H., Lee S. K., *Eur. J. Nucl. Med.*, 28 (2001) 489.
7 Muzzarelli R. A. A., *Cell Mol. Life Sci.*, 53 (1997) 131–140.
8 Koga D., *Adv. Chitin Sci.*, 3 (1998) 16.
9 He P., Davis S. S., Illum L., *Int. J. Pharm.*, 166 (1998) 75.
10 Calvo P., Vila-Jato J. L., Alonso M. J., *Int. J. Pharm.*, 153 (1997) 41.
11 Biagini G., Muzzarelli R. A. A., Giardino R., Castaldini C., in: C. J. Brine, P. A. Sandford, J. P. Zikakis (Eds.), Advances in Chitin and Chitosan, vol. 1, Elsevier Sci., Barking, 1992, pp. 16.
12 Ueno H., Mori T., Fujinaga T., *Adv. Drug Deliv. Rev.*, 52 (2001) 105.
13 Felt O., Carrel A., Baehni P., Buri P., Gurny R., *J. Ocul. Pharmacol. Ther.*, 16 (2000) 261.
14 Liu X. F., Guan Y. L., Yang D. Z., Li Z., Yao K. D., *J. Appl. Polym. Sci.*, 79 (2001) 1324.
15 Bruijn J. D. de, Dekker D., Brink I. van der, 23rd Annual Meeting of the Society for Biomaterials, April 30–May 4, New Orleans, Louisiana, USA, 1997, p. 51.
16 Heyhoe F. G. J., Quaglino D., Hematological Cytochemistry, Churchill Livingstone, London, 1980.
17 Riggs B. L., Melton L. J. III (Eds.), Osteoporosis: Etiology, Diagnosis, and Management, Lippincott-Raven Publ., Philadelphia, 1995.
18 Lahiji A., Sohrabi A., Hungerford D. S., Frondoza C. G., *J. Biomed. Mater. Res.*, 51 (2000) 586.